Eur. Phys. J. D **41**, 447–454 (2007)
DOI: 10.1140/epjd/e2006-00261-5

THE EUROPEAN PHYSICAL JOURNAL D

Femtosecond laser pulse train effect on Doppler profile of cesium resonance lines

N. Vujičić[a], S. Vdović, D. Aumiler, T. Ban, H. Skenderović, and G. Pichler

Institute of Physics, Bijenička 46, Zagreb, Croatia

Received 27 July 2006
Published online 8 December 2006 –

Abstract. We present direct observation of the velocity-selective optical pumping of the Cs ground state hyperfine levels induced by the femtosecond (fs) laser oscillator centered at either D2 ($6\ ^2S_{1/2} \rightarrow 6\ ^2P_{3/2}$, 852 nm) or D1 ($6\ ^2S_{1/2} \rightarrow 6\ ^2P_{1/2}$, 894 nm) cesium line. We utilized previously developed modified direct frequency comb spectroscopy (DFCS) which uses a fixed frequency comb for the excitation and a weak cw scanning probe laser centered at the ^{133}Cs $6\ ^2S_{1/2} \rightarrow 6\ ^2P_{3/2}$ transition (D2 line) for ground levels population monitoring. The frequency comb excitation changes the usual Doppler absorption profile into a specific periodic, comblike structure. The mechanism of the velocity selective population transfer between the Cs ground state hyperfine levels induced by fs pulse train excitation is verified in a theoretical treatment of the multilevel atomic system subjected to a pulse train resonant field interaction.

PACS. 32.80.Qk Coherent control of atomic interactions with photons – 42.50.Gy Effects of atomic coherence on propagation, absorption, and amplification of light; electromagnetically induced transparency and absorption

1 Introduction

Mode-locked, phase-stabilized femtosecond (fs) lasers with high repetition rates produce stabilized wide-bandwidth optical frequency combs [1]. It is possible to directly reference the comb spacing and position to the microwave cesium time standard, thereby determining the absolute frequencies of all comb lines. Such series of secondary reference lines that may be extended across the optical spectrum brought a revolutionary advance in metrology [2], optical frequency synthesis [3] and spectroscopy [4].

The high-resolution frequency comb spectroscopy of one- and two-photon transitions in laser-cooled and trapped rubidium atoms was reported in [5–8]. In these experiments frequency comb frequency offset could be varied. The one-photon signal was observed whenever one of the laser modes was resonant with a transition frequency of the atomic system. In the case of the two-photon transitions the counter propagating beams were used. Thus, several hundred thousand comb line-pairs with the same sum frequency contributed to the two-photon transition. The authors of reference [6] reported about unification of the fs comb time and frequency domain. As a result, a direct frequency comb spectroscopy (DFCS) was developed, allowing simultaneous investigation of the time-resolved atomic dynamic and spectral probing in the frequency domain. In systems with relaxation times larger than the laser repetition period, the medium accumulates excitation in the form of excited-state populations and coherences [9]. The authors emphasize the necessity of considering accumulative effects for a full explanation of the coherent control signal obtained from the rubidium vapor was demonstrated. The fs-pulse train effects in two- and three-level rubidium atoms were investigated experimentally and theoretically [10,11]. Recently, we investigated fs-pulse train effects in four- and six-level rubidium atoms and reported about direct observation of the velocity-selective optical pumping of the Rb ground state hyperfine levels [12,13].

We might proceed to search for new insights by keeping the repetition rate constant and testing other stable or unstable alkali isotopes with different hyperfine structure. In the present paper we demonstrate that the modified DFCS can be equally well applied to cesium atoms. The velocity-selective optical pumping of the Cs ground-state hyperfine levels induced by the femtosecond (fs) laser oscillator centered at either D2 ($6\ ^2S_{1/2} \rightarrow 6\ ^2P_{3/2}$, 852 nm) or D1 ($6\ ^2S_{1/2} \rightarrow 6\ ^2P_{1/2}$, 894 nm) cesium line was observed. Femtosecond pulse-train excitation leads to population and coherence accumulation effects, which give rise to a velocity-dependent excitation of the Doppler-broadened atomic system, resulting in the velocity-selective optical pumping mechanism. We investigate the ^{133}Cs $6\ ^2S_{1/2}$ hyperfine-level population by monitoring the $6\ ^2S_{1/2} \rightarrow 6\ ^2P_{3/2}$ probe cw laser absorption. The interaction of

[a] e-mail: natasav@ifs.hr

the inhomogeneously broadened six- and four-level cesium atom with the fs pulse train was theoretically treated. Theoretical modeling was carried out utilizing standard density matrix formalism, references [11,13,14].

2 Experiment

We have used experimental ideas developed in our previous measurements of the rubidium optical frequency comb. The experimental setup is, in all its essential parts, analogous with the one presented in references [12,13]. A Tsunami mode-locked Ti:sapphire laser with ∼100 fs pulses and a pulse repetition of 80 MHz generated the frequency comb which was fixed during the experiment. The peak wavelength of the pulse was centered at either ^{133}Cs 6 ^{2}S$_{1/2}$ → 6 ^{2}P$_{3/2}$ transition at 852 nm (D2 resonance line) or at ^{133}Cs 6 ^{2}S$_{1/2}$ → 6 ^{2} P$_{1/2}$ transition at 894 nm (D1 resonance line). Due to the substantial wavelength separation, femtosecond laser average power was not equal for two coupling wavelengths. The average power, measured at the entrance of a cesium cell, was 430 mW for fs laser tuned to 852 nm and for 894 nm case it was reduced down to 220 mW. The spectral full width at half maximum (FWHM) was around 10 nm (9 nm) when fs laser was centered at 852 nm (894 nm). The fs laser beam was focused with a $f = 1$ m lens into the sample cell producing a beam waist of about 300 μm, similar to the probe beam waist reduced using an iris. Scanning of the ^{133}Cs 6 ^{2}S$_{1/2}$ → 6 ^{2}P$_{3/2}$ hyperfine ground levels absorption profiles was obtained using the ECDL diode laser with linewidth of <1 MHz tuned to 852 nm with a mode hop free tuning range of about 15 GHz. Its frequency was scanned across the Doppler-broadened profile at a 25 MHz/ms scanning rate. Probe laser (ECDL) field power was reduced using a neutral density filter down to ∼2 μW/mm^2 (measured before entering the sample cell) to avoid saturation effects. The cesium cell with dimensions of 2.5 cm in diameter and 5.0 cm in length was placed inside the Plexiglas container. The signal acquisition was composed of one Hamamatsu Si fast photodiode connected to the digital storage oscilloscope (Tektronix TDS5104).

The photodiode was placed at the distance of about 7 m from the cell in order to spatially separate the fs and probe beams. Additionally, the probe beam polarization was changed by using the $\lambda/2$ plate and placing an analyzer before the detector. In that manner we were able to substantially reduce the presence of the fs laser signal and to observe only the probe absorption modified by the velocity-selective optical pumping induced by the frequency comb excitation.

3 Theory

Theoretical modeling of the fs-pulse train interaction with the Doppler-broadened cesium vapor was carried out utilizing standard density-matrix analysis [11–14]. We start from the Liouville equation for the density-matrix elements $\rho_{k,l}$ ($k = 1, 2$ and $l = 3$, 4, 5, 6 for lower and upper state, respectively):

$$\frac{d\rho_{kl}}{dt} = -\frac{i}{\hbar}\langle k\,|[H,\rho]|\,l\rangle - \frac{1}{T_{kl}}\rho_{kl}. \tag{1}$$

The Hamiltonian of the system $H = H_0 + H_{\rm int}$ consists of two parts: H_0 is the Hamiltonian of the free atom and $H_{\rm int} = -\mu_{kl}E_T(t)$ represents the interaction of the atom with the laser electric field $E_T(t)$. The values for the effective dipole moment μ_{kl} of electronically allowed transitions ($F_g \to F_e = F_g$, $F_g \pm 1$) were taken from [15]. The detailed description of the electric field $E_T(t)$ of the pulse train together with the related notation is given in our previous work, reference [13].

The Liouville equation is modified with the term that takes into account the repopulation of the ground states due to the spontaneous decay from the excited states and with the collisional mixing term, as well. The collisional mixing term Π describes the thermalization of the hyperfine levels and it can be calculated, according to [14], as a product of atomic number density N, the collision cross section σ and the average atom velocity υ. For cesium vapor $\sigma = 2.35 \times 10^{-13}$ cm^2 [16], whereas N and υ are temperature dependent. Under the experimental conditions, at room temperature ($T = 296$ K), their values are $\upsilon = 193$ m/s and $N = 1.22 \times 10^{16}$ m^{-3} which yields $\Pi = 55.4$ Hz, which is even five orders of magnitude smaller than the population and coherence relaxation rates. This explains the existence of the optical pumping of the ground hyperfine states. As it was noticed before, since the pulse repetition period $T_R = 12.5$ ns is smaller than the relaxation times of the system, the system can never completely relax between two consecutive laser pulses which leads to the accumulation of the coherences and the excited-state populations.

The population decay rates ($\Gamma_{kl} = 1/T_{kl}$) were calculated from the cesium upper states (6 ^{2}P$_{1/2,3/2}$) population lifetimes T, which amount 30.47 ns and 34.89 ns for 6 ^{2}P$_{3/2}$ and 6 ^{2}P$_{1/2}$ excited states, respectively. The coherence decay rates (γ_{kl}) for the 4-level system are calculated according to [14]:

$$\gamma_{12} = \Pi \tag{2a}$$

$$\gamma_{13} = \gamma_{23} = \frac{\Gamma_{31}}{2} + \frac{\Gamma_{32}}{2} + \Pi \tag{2b}$$

$$\gamma_{14} = \gamma_{24} = \frac{\Gamma_{41}}{2} + \frac{\Gamma_{42}}{2} + \Pi \tag{2c}$$

$$\gamma_{34} = \frac{\Gamma_{41}}{2} + \frac{\Gamma_{42}}{2} + \frac{\Gamma_{31}}{2} + \frac{\Gamma_{32}}{2} + \Pi. \tag{2d}$$

Similarly, for the 6-level system there are 15 coherence decay rates:

$$\gamma_{12} = \Pi \tag{3a}$$

$$\gamma_{13} = \gamma_{23} = \frac{\Gamma_{31}}{2} + \Pi \tag{3b}$$

$$\gamma_{14} = \gamma_{24} = \frac{\Gamma_{41}}{2} + \frac{\Gamma_{42}}{2} + \Pi \tag{3c}$$

$$\gamma_{15} = \gamma_{25} = \frac{\Gamma_{51}}{2} + \frac{\Gamma_{52}}{2} + \Pi \tag{3d}$$

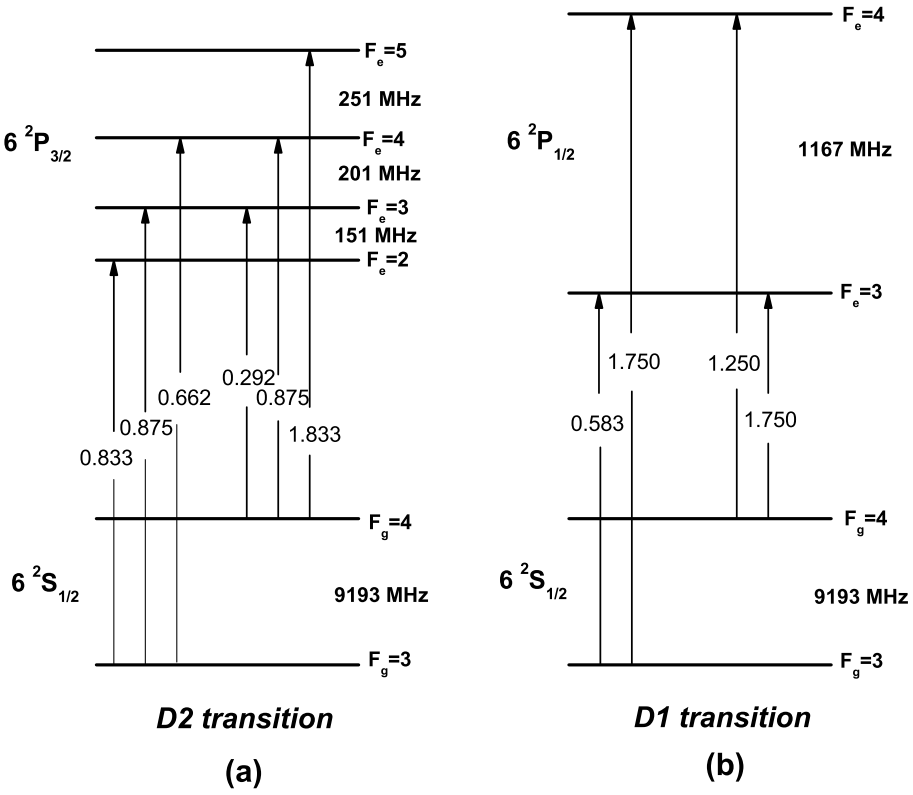

Fig. 1. Cesium D2 transition (six-level) (a) and D1 transition (four-level), (b) hyperfine structure scheme.

$$\gamma_{16} = \gamma_{26} = \frac{\Gamma_{62}}{2} + \Pi \tag{3e}$$

$$\gamma_{34} = \frac{\Gamma_{41}}{2} + \frac{\Gamma_{42}}{2} + \frac{\Gamma_{31}}{2} + \Pi \tag{3f}$$

$$\gamma_{35} = \frac{\Gamma_{51}}{2} + \frac{\Gamma_{52}}{2} + \frac{\Gamma_{31}}{2} + \Pi \tag{3g}$$

$$\gamma_{36} = \frac{\Gamma_{62}}{2} + \frac{\Gamma_{31}}{2} + \Pi \tag{3h}$$

$$\gamma_{45} = \frac{\Gamma_{51}}{2} + \frac{\Gamma_{52}}{2} + \frac{\Gamma_{41}}{2} + \frac{\Gamma_{42}}{2} + \Pi \tag{3i}$$

$$\gamma_{46} = \frac{\Gamma_{62}}{2} + \frac{\Gamma_{41}}{2} + \frac{\Gamma_{42}}{2} + \Pi \tag{3j}$$

$$\gamma_{56} = \frac{\Gamma_{62}}{2} + \frac{\Gamma_{51}}{2} + \frac{\Gamma_{52}}{2} + \Pi. \tag{3k}$$

From equation (1) a system of ten (twenty one) coupled differential equations for the slowly varying density-matrix elements can be obtained for the four levels ^{133}Cs 6 ^{2}S$_{1/2}$ $\rightarrow$ 6 ^{2}P$_{3/2}$ (six levels ^{133}Cs 6 ^{2}S$_{1/2}$ $\rightarrow$ 6 ^{2}P$_{1/2}$) transition. The theoretical model is analogous to the one employed in our previous paper [13] where the interaction of the fs pulse train with four- and six-level Rb system was considered. There, the complete set of the differential equations was presented, including the additional terms (repopulation terms and collisional mixing term) with detailed description and extended explanation. Six-level Cs system (D2 transition) comprises two ground (F_g = 3, 4) and four excited (F_e = 2, 3, 4, 5) hyperfine levels, Figure 1a, whereas the four-level Cs system (D1 transition) consists of two ground (F_g = 3, 4) and two excited (F_e = 3, 4) hyperfine levels, Figure 1b. The population of the kth atomic level is given by the diagonal density-matrix element ρ_{kk}, whereas off-diagonal elements $\sigma_{kl} = \rho_{kl}e^{-i\omega_L t}$ represent the slowly varying envelope of coherences.

The inhomogeneous Doppler broadening of about 380 MHz for cesium resonance lines at room temperature is significantly larger than the homogeneous broadening. As a result, the atomic transition frequency ω_{ge} must be replaced with a $\omega'_{ge} = \omega_{ge} + \vec{k}\cdot\vec{v}$, where $\vec{k}$ is the laser wave vector and $\vec{v}$ is the atomic velocity vector. The atoms with different velocities correspond to different detuning, $\delta = \vec{k}\cdot\vec{v}$ so for given ω_n and given $F_g \rightarrow F_e$ hyperfine transition there is a specific velocity group (δ_n detuning) which fulfills $\omega_n = \omega'_{ge}$ resonant condition. Since the pulse train frequency spectrum consists of a comb of laser modes separated by $1/T_R$ (80 MHz), the resonant condition is also satisfied for the atoms with detuning $\delta = \delta_n \pm 2\pi k/T_R$, where k is a positive integer. Consequently, different velocity groups of the atoms can be distinguished by means of the excitation (accumulation) process due to the interaction with the frequency comb. As a result, the velocity-selective optical pumping of the Cs ground state hyperfine levels and the velocity-selective population in excited hyperfine levels is observed.

The time evolution of the atomic level populations and coherences was obtained solving the system of coupled differential equations for the slowly varying density-matrix elements. The system of differential equations was integrated using a standard fourth-order Runge-Kutta method. From the calculated values of the hyperfine

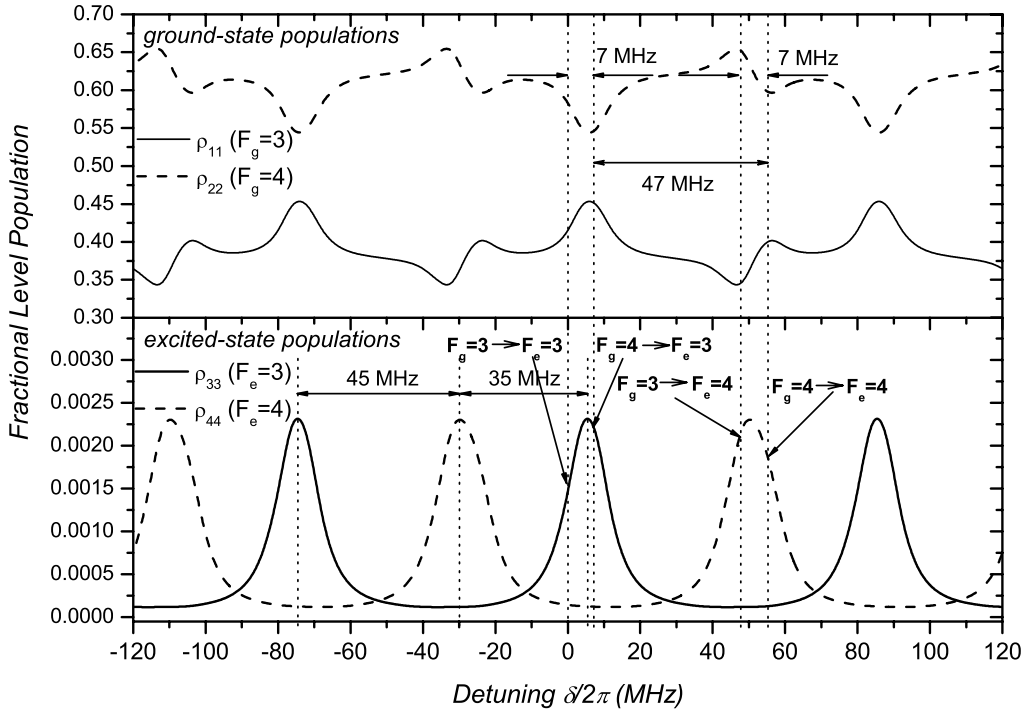

Fig. 2. Calculated ground (ρ_{11}, ρ_{22}) and excited (ρ_{33}, ρ_{44}) state cesium hyperfine-level populations for different atomic velocity groups in the case of 6 $^2S_{1/2} \rightarrow 6\ ^2P_{1/2}$ fs-laser excitation (894 nm). Only a central part of the Doppler-broadened profile is presented.

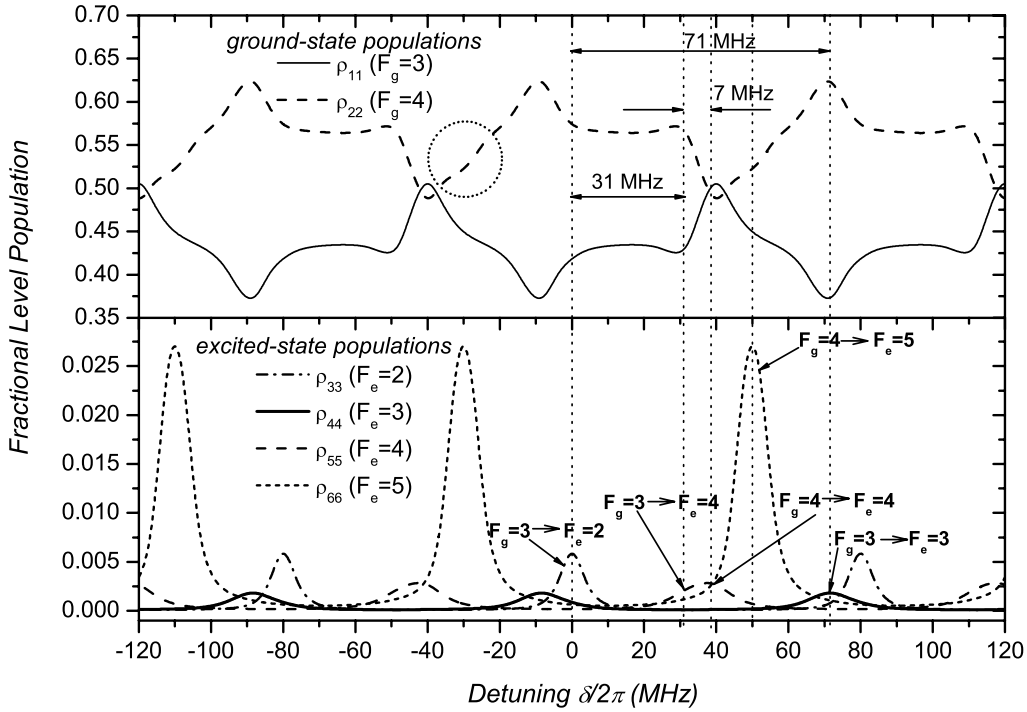

Fig. 3. Calculated ground (ρ_{11}, ρ_{22}) and excited (ρ_{33}, ρ_{44}, ρ_{55}, ρ_{66}) state cesium hyperfine-level populations for different atomic velocity groups in the case of 6 $^2S_{1/2} \rightarrow 6\ ^2P_{3/2}$ fs-laser excitation (852 nm). Only a central part of the Doppler-broadened profile is presented.

ground state populations ρ_{11} and ρ_{22} the theoretical simulation of the measured absorption lines can be obtained. For each hyperfine transition, we calculated the convolution of the velocity distribution of the ground state population with the Lorentzian profile of natural linewidth. The absorption lines were calculated by adding the contributions of three hyperfine components for the D2 transition case, i.e. two hyperfine components for the D1 transition at 894 nm.

4 Results and discussion

The calculated hyperfine ground- and excited-state levels populations for different atomic velocity groups (different detuning δ) are presented in Figures 2 and 3 for D1 transition (6 $^2S_{1/2} \rightarrow 6\ ^2P_{1/2}$) and D2 transition (6 $^2S_{1/2} \rightarrow 6\ ^2P_{3/2}$), respectively. The level populations vary periodically with a period of 80 MHz, which is a direct consequence of the comb frequency spectrum. For

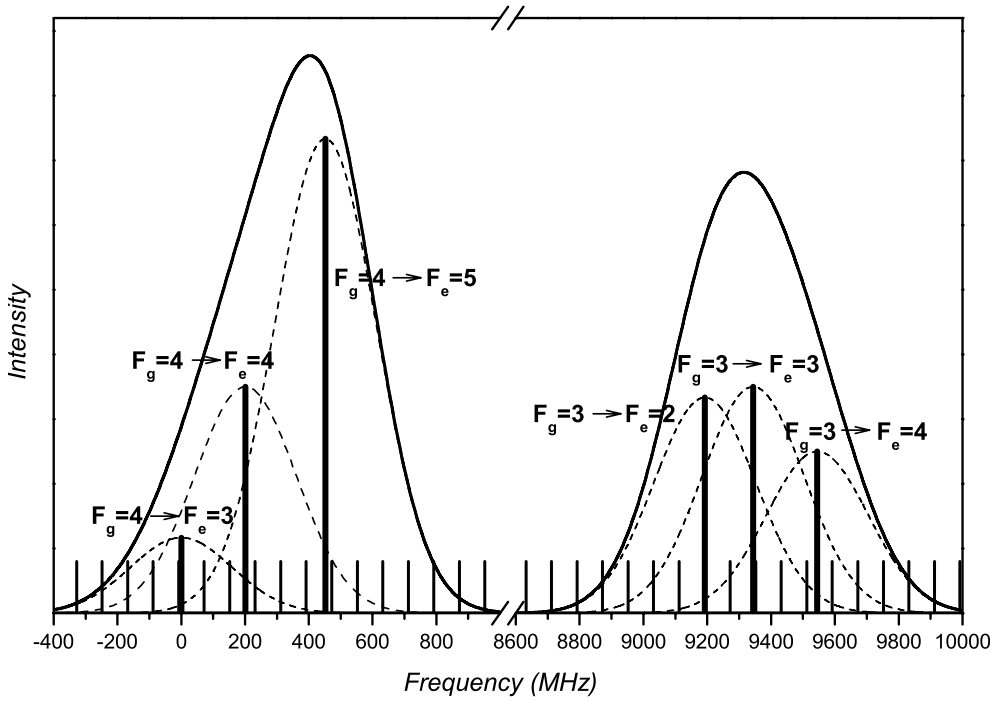

Fig. 4. The Doppler-broadened cesium 6 $^2S_{1/2}(F_g) \rightarrow 6\ ^2P_{3/2}$ ($F_e = F_g,\ F_g \pm 1$) hyperfine transitions together with the frequency comb lines structure separated by 80 MHz. The fs laser frequency ω_L is centered at 6 $^2S_{1/2}(F_g = 3) \rightarrow 6\ ^2P_{3/2}$ ($F_e = 2$) transition.

the ^{133}Cs 6 $^2S_{1/2} \rightarrow 6\ ^2P_{3/2}$ transition (D2), the calculations were performed for the laser electric field amplitude 5.2×10^5 V/m, $T_R = 12.5$ ns, $\Phi_R = 0$, and ω_L equal to the 6 $^2S_{1/2}$ ($F_g = 3$) $\rightarrow 6\ ^2P_{3/2}$ ($F_e = 2$) transition frequency. In the case of the ^{133}Cs 6 $^2S_{1/2} \rightarrow 6\ ^2P_{1/2}$ transition (D1), related average power was reduced down to 220 mW, as a consequence of the decreased laser electric field amplitude of about 3.2×10^5 V/m. The other parameters remained the same, i.e., $T_R = 12.5$ ns, $\Phi_R = 0$ and ω_L equals to the 6 $^2S_{1/2}(F_g = 3) \rightarrow 6\ ^2P_{1/2}(F_e = 3)$ transition frequency.

In the case of 6 $^2S_{1/2} \rightarrow 6\ ^2P_{1/2}$ excitation, the $F_g = 3$ ground level population (ρ_{11}) in one 80 MHz period exhibits two maxima and one minimum, Figure 2. The minimum formed in ρ_{11} corresponds to the maximum in ρ_{22} and vice versa. When the laser is resonant with the $F_g = 3 \rightarrow F_e = 3$ transition (minimum in ρ_{11}), it is 7 MHz off-resonance with the respect to the $F_g = 4 \rightarrow F_e = 3$ transition (maximum in ρ_{11}, larger minimum in ρ_{22}). The reason for such behavior lies in the fact that the 6 $^2S_{1/2}$ hyperfine splitting is 9193 MHz, nearly the multiple of 80 MHz. The $F_g = 4 \rightarrow F_e = 3$ transition is responsible for the maximum in the ρ_{33} fractional level population. The $F_g = 3 \rightarrow F_e = 3$ transition, due to the significantly lower transition probability does not have such impact on ρ_{33} creation. Two maxima in ρ_{11} (minima in ρ_{22}) are separated by $\delta = 47$ MHz, Figure 2. This comes as a result of the 1167 MHz energy splitting between the cesium excited-state hyperfine energy levels ($F_e = 3$ and $F_e = 4$). The $F_g = 3 \rightarrow F_e = 4$ transition (minimum in ρ_{11}) is also 7 MHz off-resonance with the respect to the $F_g = 4 \rightarrow F_e = 4$ transition (smaller maximum in ρ_{11}, minimum in ρ_{22}). As a result, due to the equal values of the relative transition probabilities (Fig. 1) and near-resonance condition, both transitions participate in the ρ_{44} level population and their contributions are difficult to distinguish. Due to the 80 MHz laser mode separation in the frequency comb spectrum, the resonance condition for the $F_g \rightarrow F_e$, $F_e \pm 1$ transition is achieved for the detuning of 47 MHz. Two consecutive maxima in the excited-state fractional level population (ρ_{33} and ρ_{44}) are separated by 35 MHz and 45 MHz, which can be also observed in Figure 5 as a double peak in each modulation of the Doppler-broadened absorption lines.

In the case of 6 $^2S_{1/2} \rightarrow 6\ ^2P_{3/2}$ excitation, the $F_g = 3$ ground level population (ρ_{11}) in one 80 MHz period exhibits one maximum and two minima, Figure 3. At the same time, one can observe one minimum and two maxima in $F_g = 4$ ground level population (ρ_{22}). The laser is resonant with the optically closed $F_g = 3 \rightarrow F_e = 2$ transition (detuning $\delta = 0$ MHz) but it does not reduce ρ_{11} due to the weak relative transition probability. For the optically closed transitions, the minimum in ρ_{11} does not lead to maximum in ρ_{22}. The reason why one cannot observe the considerable decrease in ρ_{11} is due to the small fractional excited-level population ρ_{33} that is around 0.5%. The similar effect was observed in rubidium [13]. The larger minimum in ρ_{11} comes as the result of the $F_g = 3 \rightarrow F_e = 3$ hyperfine transition, which is 71 MHz detuned with respect to the 80 MHz separation in the comb spectrum ($F_e = 2$ and $F_e = 3$ have energy separation of 151 MHz). Smaller minimum in ρ_{11} comes as a result of $F_g = 3 \rightarrow F_e = 4$ transition, although the ρ_{55} excited-state population is mainly created due to the $F_g = 4 \rightarrow F_e = 4$ transition which has larger transition probability (minimum in ρ_{22}). Since the $F_g = 3, 4 \rightarrow F_e = 3, 4$ transitions are optically open ones, they induce strong optical pumping of

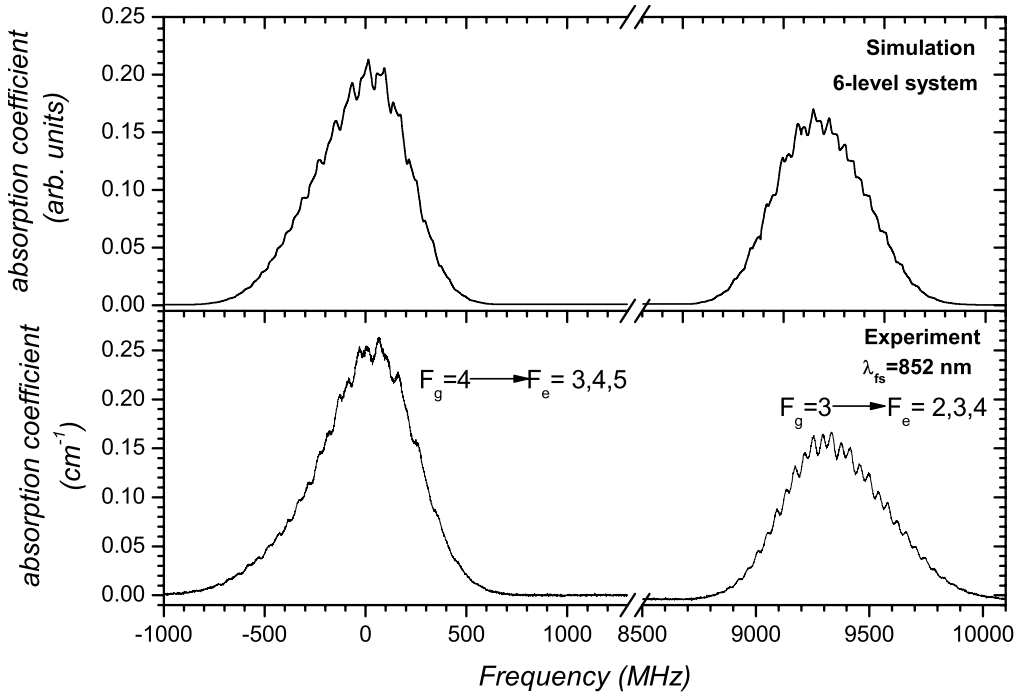

Fig. 5. The comparison of the measured and simulated ^{133}Cs $6\ ^2S_{1/2} \rightarrow 6\ ^2P_{3/2}$ hyperfine absorption line profiles in the case of $6\ ^2S_{1/2} \rightarrow 6\ ^2P_{3/2}$ fs-laser excitation.

the ground hyperfine-level populations. Hence, when the resonant condition is fulfilled for one of these transitions, the minimum in ρ_{11} creates the maximum in ρ_{22}, and vice versa. The transitions with the same upper hyperfine level, such as $F_g = 3 \rightarrow F_e = 4$ transition (minimum in ρ_{11}) and $F_g = 4 \rightarrow F_e = 4$ transition (larger minimum in ρ_{22}), are 7 MHz off-resonance as a consequence of the $6\ ^2S_{1/2}$ hyperfine splitting (9193 MHz), which is nearly the multiple of 80 MHz. Due to the weak relative transition probability, the $F_g = 4 \rightarrow F_e = 3$ transition does not lead to the additional depletion of ρ_{22} population. $F_g = 4 \rightarrow F_e = 5$ transition is optically closed one and it should create minimum in ρ_{22}, without relating maximum in ρ_{11}. This minimum in ρ_{22} is barley discernible (it is marked with the circle in Fig. 3). The excited-level populations are below 1%, except for the $F_e = 5$, which value is 2.7% (at the maximum), due to the optically closed transition with a strong transition probability. Low power of the femtosecond pumped laser is additional reason for small fractional level population of excited-states. Since the collisional mixing term is five orders of magnitude smaller than the population and coherence relaxation rates, the significant optical pumping of the ground hyperfine states is achieved.

From the discussion given above it is obvious that the ^{133}Cs ground- and excited-state hyperfine level populations are determined by the hyperfine energy splittings and relative transition probabilities, resulting with a periodic behavior given by the mode separation in the frequency comb (periodically with 80 MHz).

The experimental observation of the hyperfine ground-state populations is achieved by monitoring the weak cw probe laser transmission. The absorption spectra consist of two lines that present the hyperfine splitting of the ground state, which amounts to 9193 MHz. Each line consists of three Doppler-broadened hyperfine transitions ($6\ ^2S_{1/2}(F_g) \rightarrow 6\ ^2P_{3/2}$ ($F_e = F_g, F_g \pm 1$)), which is illustrated in Figure 4. The frequency comb is also presented in Figure 4 with the central laser frequency ω_L equal to $6\ ^2S_{1/2}$ ($F_g = 3$) $\rightarrow 6\ ^2P_{3/2}$ ($F_e = 2$) transition frequency, corresponding to the calculations presented in Figure 3. In Figures 5 and 6 we present the measured and simulated ^{133}Cs absorption lines in the cases of $6\ ^2S_{1/2} \rightarrow 6\ ^2P_{3/2}$ and $6\ ^2S_{1/2} \rightarrow 6\ ^2P_{1/2}$ fs laser excitations, respectively. The theoretical simulations of the measured absorption spectra were calculated utilizing ρ_{11} and ρ_{22} hyperfine ground-level populations, shown in Figures 2 and 3.

By changing the fs-laser excitation from $6\ ^2S_{1/2} \rightarrow 6\ ^2P_{3/2}$ to $6\ ^2S_{1/2} \rightarrow 6\ ^2P_{1/2}$, we observed characteristic changes both in the intensity and shape of the modulations in cesium absorption profiles. The stronger modulations were observed in the case when the fs-laser was tuned on $6\ ^2S_{1/2} \rightarrow 6\ ^2P_{3/2}$ transition (430 mW), due to the higher average power than for the $6\ ^2S_{1/2} \rightarrow 6\ ^2P_{1/2}$ case (220 mW). As was reported before in reference [13], the relative modulation intensities depend on the fs-laser power, i.e. increasing the laser power increases the modulation intensities. Any additional power increase results in the saturation of the modulation intensities. In our experimental conditions the fs-laser powers were below that value.

5 Conclusion

In conclusion, we have presented an experimental and theoretical study of the resonant excitation of cesium atoms

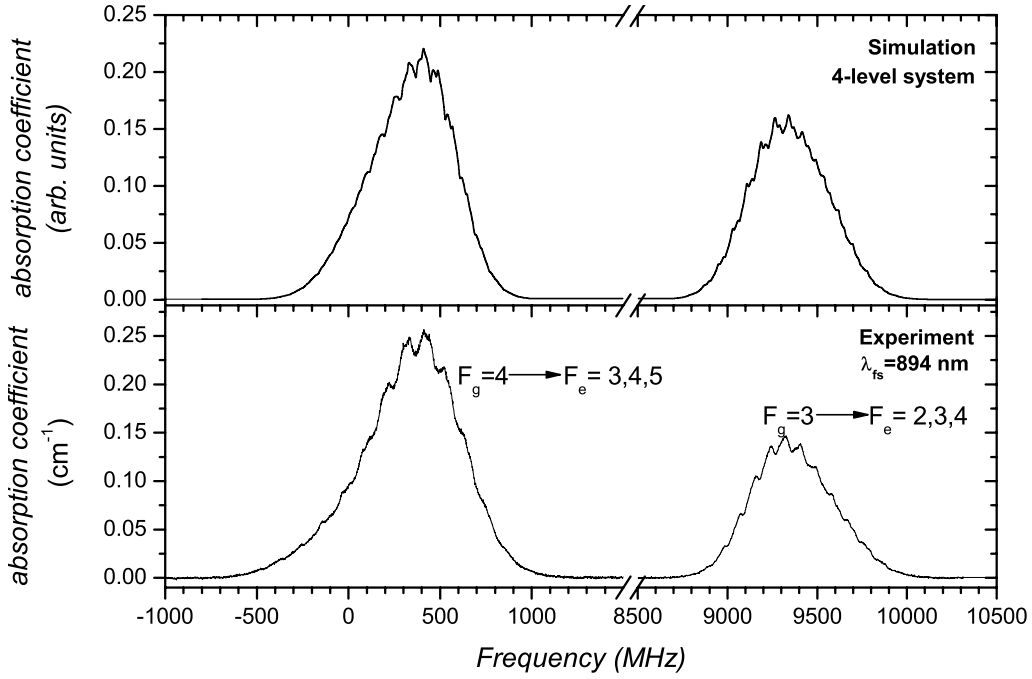

Fig. 6. The comparison of the measured and simulated ^{133}Cs 6 $^2S_{1/2} \rightarrow 6\ ^2P_{3/2}$ hyperfine absorption line profiles in the case of 6 $^2S_{1/2} \rightarrow 6\ ^2P_{1/2}$ fs-laser excitation.

with the fs-pulse train treated in frequency domain. The ^{133}Cs (6 $^2P_{1/2,3/2}$) excited atomic states have relaxation times greater than the fs-laser repetition period. In the time domain this leads to population and coherence accumulation effects, whereas in the frequency domain it corresponds to the interaction of the cesium atoms with the fs-frequency comb. As a result, we were able to observe a velocity-selective, comblike excited-state hyperfine-level populations and, simultaneously, velocity-selective pumping of the ground-state hyperfine levels.

The modulations in the 6 $^2S_{1/2} \rightarrow 6\ ^2P_{3/2}$ hyperfine absorption line profiles were observed utilizing a simple experimental apparatus. The monochromatic weak cw scanning probe laser was employed for ground-level population monitoring, while the 6 $^2S_{1/2} \rightarrow 6\ ^2P_{1/2,3/2}$ excitations were achieved with the fixed-frequency comb. The fs-pulse train excitation of a Doppler-broadened cesium vapor was theoretically treated in the context of the density-matrix formalism. By comparing the experimental results with the simulated 6 $^2S_{1/2} \rightarrow 6\ ^2P_{3/2}$ absorption profiles we can observe satisfactory agreement.

This work confirms that the modified DFCS developed on ^{85}Rb and ^{87}Rb atoms can be applied on cesium atom, as well. Although these two atomic systems are basically different, the experimental results and the theoretical simulations give reproducible results. The cesium atom serves as the primary standard of time and it plays an important role in many experiments on laser cooling, trapping, atom interferometry and the precise measurements, therefore it presents an interesting subject for the further investigations. It would be interesting to investigate the same effect on cesium with cw laser fixed on D1 line (894 nm) due to the relatively simple transition hyperfine 4-level structure and the large ground- and excite-state hyperfine splittings (over 1 GHz).

We foresee a prospect of our present work in an attempt to directly select only the central velocity group with $\vec{v} = 0$ m/s. This may lead to an effective cooling of the sample. Furthermore, if we take six different fs laser beams, at right angle to each other, we might possibly bring about a specific cooling effect to the sample in 3 dimensions. This scheme, already well-known in the magneto-optical trap (MOT) can be employed here, with essentially the same result — the preparation of ultracold atom sample. In addition to this, some of the frequency comb lines may become active in photoassociation process, thus simultaneously forming ultracold alkali molecules. Making and trapping ultracold molecules is certainly one of the most important and very attractive goals of our investigations.

We acknowledge the support from the Ministry of Science, Education and Sports of Republic of Croatia (Projects 0035002), European Commission Research Training Network on Cold Molecules (FW-5) and Alexander von Humboldt Foundation (Germany).

References

1. S.T. Cundiff, J. Ye, Rev. Mod. Phys. **75**, 325 (2003)
2. S. Witte, R.Th. Zinkstok, W. Udbachs, W. Hogervorst, K.S.E. Eikema, Science **307**, 400 (2005)
3. K.R. Vogel, S.A. Diddams, C.W. Gates, E.A. Curtis, R.J. Rafac, W.M. Itano, J.C. Bergquist, W. Fox, W.D. Lee, J.S. Wells, L. Hollberg, Opt. Lett. **26**, 102 (2001)
4. Th. Udem, J. Reichert, R. Holzwarth, T.W. Hänsch, Phys. Rev. Lett. **82**, 3568 (1999)
5. M.J. Snadden, A.S. Bell, E. Riis, A.I. Ferguson, Opt. Commun. **125**, 70 (1996)

6. A. Marian, M.C. Stowe, J.R. Lawall, D. Felinto, J. Ye, Science **306**, 2063 (2004)
7. H.-C. Chui, M.-S. Ko, Y.-W. Liu, J.-T. Shy, Opt. Lett. **30**, 842 (2005)
8. A. Marian, M.C. Stowe, D. Felinto, J. Ye, Phys. Rev. Lett. **95**, 023001 (2005)
9. D. Felinto, C.A.C. Bosco, L.H. Acioli, S.S. Vianna, Phys. Rev. A **64**, 063413 (2001)
10. D. Felinto, C.A.C. Bosco, L.H. Acioli, S.S. Vianna, Opt. Commun. **215**, 69 (2003)
11. D. Felinto, L.H. Acioli, S.S. Vianna, Phys. Rev. A **70**, 043403 (2004)
12. D. Aumiler, T. Ban, H. Skenderović, G. Pichler, Phys. Rev. Lett. **95**, 233001 (2005)
13. T. Ban, D. Aumiler, H. Skenderović, G. Pichler, Phys. Rev. A **73**, 043407 (2006)
14. J.R. Boon, E. Zekou, D.J. Fulton, M.H. Dunn, Phys. Rev. A **57**, 1323 (1998)
15. D.A. Steck, cesium D line data, `http://steck.us/alkalidata`
16. I. Estermann, S.N. Foner, O. Stern, Phy. Rev. **71**, 250 (1947)